CERN-SPSC-2013-024 / SPSC-EOI-010
January 3, 2014

Answers to the questions from the SPSC concerning the SPSC-EOI-010

W. Bonivento[1,2], A. Boyarsky[3], H. Dijkstra[2], U. Egede[4], M. Ferro-Luzzi[2], B. Goddard[2], A. Golutvin[4], D. Gorbunov[5], R. Jacobsson[2], J. Panman[2], M. Patel[4], O. Ruchayskiy[6], T. Ruf[2], N. Serra[7], M. Shaposhnikov[6], D. Treille[2 (‡)]

[1] *Sezione INFN di Cagliari, Cagliari, Italy*
[2] *European Organization for Nuclear Research (CERN), Geneva, Switzerland*
[3] *Instituut-Lorentz for Theoretical Physics, Universiteit Leiden, Niels Bohrweg 2, Leiden, The Netherlands*
[4] *Imperial College London, London, United Kingdom*
[5] *Institute for Nuclear Research of the Russian Academy of Sciences (INR RAN), Moscow, Russia*
[6] *Ecole Polytechnique Fédérale de Lausanne (EPFL), Lausanne, Switzerland*
[7] *Physik-Institut, Universität Zürich, Zürich, Switzerland*
(‡) *retired*

1 Introduction

This document represents a status report concerning the questions of the SPSC. More information can be found in the slides (see https://indico.cern.ch/conferenceDisplay.py?confId=287749) presented to the referees at the meeting on the 11th December 2013.

The physics case has been significantly elaborated beyond the EoI. The νMSM imposes the most severe constraints on the Heavy Neutral Lepton (HNL) parameter space. The responses to Questions 1 and 2 describe a rich class of models beyond the νMSM with HNLs at the Fermi scale, and a number of examples of low energy SUSY. In particular, the search for sgoldstinos will provide constraints on the scale of the SUSY breaking.

The proposed experiment does not address neutrino physics. However there is an attractive possibility in studying the properties of the tau neutrino which is produced with a kinematics similar to the HNLs.

The responses to Questions 3 to 6 reflect our current understanding. We have studied additional decay modes and found that the proposed experiment with the current choice of technologies will also have a very good sensitivity to modes with electrons, photons, and π^0 mesons in the final states. We have demonstrated that there is a viable solution with both a passive, and with a combination of an active and a passive muon shield. However the final optimization remains to be completed. In particular, further progress requires more detailed simulations of the muon interactions in the material close to the decay volume, as well as a better understanding of the background sources.

The response to Question 8 containes a very preliminary cost estimate of the entire facility required for the proposed experiment.

At this stage our efforts to strengthen the collaboration beyond the list shown at the open SPSC session on October 23, 2013 has been concentrated on raising interest in the scientific aspects. The response to Question 9 presents a list of seminars and conference talks given by the proponents.

2 Q1: Can other physics be measured with the experiment as proposed in the EoI? What is the potential to extend the use of such a facility beyond the search for neutral leptons in the 0.5-2 GeV range?

The proposed experiment is ideally suited for studying interactions of tau neutrinos and for searching for very weakly interacting yet unstable particles with masses ranging from 100 MeV up to 2 GeV.

2.1 Physics with tau neutrinos

The optimal design of the beam line for the search for HNLs consists of maximizing the production of charmed mesons in the proton beam dump and minimizing the production of "conventional" neutrinos from light meson decays. The same design criteria optimize the yield of tau neutrinos that are produced in D_s decays. It is therefore natural to consider the opportunities offered by this beam for ν_τ physics.

The following assumes that a compact tau neutrino detector is located centred on the beam axis directly downstream of the muon shield and upstream of the HNL decay volume. Estimates of the rates can be obtained from the DONUT experiment performed at the FNAL Tevatron. The DONUT detector was exposed to a neutrino beam produced by 800 GeV protons on a tungsten dump (proton target), and was located at a 35 m distance from the dump. The detector measured a total of 9 candidate events including an estimated number of

1.5 background events from charm production in an exposure of 3.54×10^{17} protons on target (pot). Scaling these numbers to a 400 GeV beam with 2×10^{20} pot requires knowledge of the relative D_s production cross-sections R_prod ($R_\mathrm{prod} = 0.36$), neutrino detector acceptance R_acc ($R_\mathrm{acc} = 0.2$), and the energy dependence of the ν_τ cross-section R_σ ($R_\sigma = 0.52$). With these numbers a scaling factor for the number of events recorded with the same target mass $R_\mathrm{specific} = R_\mathrm{pot}\, R_\mathrm{prod}\, R_\mathrm{acc}\, R_\sigma \approx 20$ is obtained using $R_\mathrm{pot} = 564$ and assuming the same reconstruction efficiency.

With a neutrino target design based on the OPERA lead/emulsion bricks, it is realistic to assume that the proposed experiment could incorporate an emulsion target of 3000 kg as compared to the total fiducial target mass of 260 kg in the DONUT experiment. The 3000 kg target would be provided by 375 bricks, each of which has a width of 12 cm, a height of 10 cm, and a thickness in the beam direction of about 8 cm. Such an emulsion target would thus accumulate 1700 observed ν_τ interactions during the full exposure. One should note that the rate estimates contain a 40% statistical uncertainty due to the small number of signal events in the DONUT experiment. It is estimated that the total number of neutrino interactions of all types is of the order of 3000 per brick. To keep the excellent pattern recognition and precision of the emulsion technique, one can tolerate ≈ 300 interactions per brick. To satisfy this constraint the target needs to be exchanged each 2×10^{19} pot (i.e. a total of ten successive targets). Such an exchange strategy would necessitate 2700 m^2 of emulsion plate, that is, only 3% of the OPERA surface.

The regular exchange also eases the requirement on the background muon flux. The optimum number of muons is driven by the need for a precise alignment of the emulsion plates. For each exposure, $10^3/\mathrm{mm}^2$ is optimal, while $10^4/\mathrm{mm}^2$ should be considered as a maximum. These numbers are very similar to the requirements of the HNL detector and appear achievable with a realistic muon shield (Sec. 5).

The interactions of the ν_τ are recognized by the τ lepton produced at the primary vertex. In the emulsion target, the τ leptons are identified by their characteristic decay topology. The main background to the τ sample comes from charmed-particle production in charged-current (CC) interactions where the primary lepton is missed. Muon identification can be achieved with a standard downstream muon identifier. Electrons are efficiently detected in the emulsion target by observation of their showers. Kinematic analysis can further reduce the background to the 10% level.

The ν_τ interactions are composed of nearly equal numbers from the two helicities. The helicity of the neutrino can be tagged by measuring the total charge of the τ decay products, which is possible for the muonic and hadronic modes in a magnetic field. While the electron decay mode is readily recognized, the charge is difficult to determine. The most economical and compact solution is to place the emulsion target inside a magnetic field and measure the charge of τ daughters with a compact emulsion spectrometer (CES) following each brick.

Each CES consists of a set of emulsion plates separated by low-density spacers and requires about 10 cm in longitudinal dimension in a field of 0.5–1 T to determine the charge of particles.

In addition to the emulsion plates, interface trackers are needed to connect the emulsion tracks with the tracks in the electronic detectors. About 10 m^2 of e.g. scintillating fibre tracker would be adequate. The emulsion target including the bricks and emulsion spectrometers fit inside a volume of 2 m^3. A magnet with such a magnetic volume is technically feasible and may even be available.

In addition to the study of ν_τ interactions, also neutrino-induced charged-current charm production can be studied. It is estimated that 10^4 candidates could be observed with negligible background. The neutrino helicity can be tagged using the primary muon charge. Such a sample would be larger than the numbers of events collected by CHORUS (2000 events), and would make it possible to study structure functions, production fractions, fragmentation functions, topological branching fractions etc. with higher precision than possible before.

The synergy of the HNL decay programme and the ν_τ programme is large:

- the beamline and proton exposure are shared;
- the muon identification for the ν_τ detector is performed by the HNL veto;
- the HNL spectrometer serves as a forward muon spectrometer for the ν_τ programme;
- the instrumentation of the ν_τ muon identifier provides additional suppression of the K^0_L background for the HNL search;
- the study of neutrino interactions in the ν_τ detector provides a measurement of the neutrinos from the charm decays in the proton dump, which is important to normalize the HNL signal, and allow calculating the backgrounds for the HNL experiment. In particular, the distribution and number of ν_e interactions give access to the normalization of charmed mesons produced in the proton beam dump.

Owing to the compact design of the ν_τ detector, the loss of acceptance for the HNL experiment is only a few % as can be seen from Figure 8.

In summary, with a modest investment and with a very small acceptance loss for the HNL experiment, it is possible to exploit the same beam line to study both τ-neutrino interactions, including a precise cross-section measurement, measurements of form factors and of the τ angular distributions, and improving limits on the anomalous magnetic moment, as well as charm production in neutrino interactions with a much larger number of events than in previous experiments such as DONUT and E531 at FNAL, and CHORUS at CERN. With the use of emulsion technology to detect ν_τ interactions, it is realistic to consider a factor of ten more target mass than DONUT and gain more than two orders of magnitude in the number of reconstructed ν_τ interactions with a total background fraction similar to DONUT.

2.2 Sensitivity to BSM physics other than HNLs

Fixed target experiments provide powerful possibilities [1] for probing *portals* to the secluded sectors, that is, renormalizable interactions between SM fields and hypothetical SM-singlets. The corresponding coupling constants are dimensionless and hence the physics may be probed equally well by both low-energy and high-energy experiments. However, given the small coupling constants and typically long lifetimes, the much higher statistics and detector configuration make fixed target experiments much more promising in this task.

Different models propose different types of portals consisting of (pseudo)scalars, neutral fermions or (axial) vectors. Below we illustrate the sensitivity of the proposed experiment by a set of examples which are widely discussed in literature and for which the hypothetical particle masses are $O(GeV)$ and production branching ratios are $O(10^{-10})$.

- Light sgoldstinos (superpartners of goldstino in SUSY): axion- and dilaton-like particles in supersymmetric extensions of the SM, see e.g. [2]. They may be produced in heavy hadron decays, e.g. $D \to \pi\, X$, and then decays into pairs of the SM particle, e.,g. $X \to \pi^+\, \pi^-$.

- Light R-parity violating neutralinos in SUSY: Heavy neutrino-like particles in supersymmetric extensions of the SM with R-parity violation, see e.g., [3]. They may be produced in heavy hadron decays, e.g. $D \to l\, \tilde{\chi}$, and then decay into three-body final states, e.g. $\tilde{\chi} \to l^+\, l^-\, \nu$.

- Light (axial) vectors in secluded dark matter models: Massive paraphotons from a hidden sector, e.g. [4]. They may be produced in heavy hadron decays, e.g. $\Sigma \to p\, V$, and then decay into pairs of the SM particle, e.g. $V \to l^+\, l^-$.

Generally speaking, the proposed experiment is sensitive to the same models as the former CHARM experiment. However, the higher statistics and better detector performance will give access to longer lifetimes and smaller couplings.

Below we discuss these three examples in more detail.

2.2.1 New scalar X: Light sgoldstinos in SUSY models

Here we discuss the physics of the *Goldstino supermultiplet* (bosons φ, fermion ψ, auxiliary field F) in which the spontaneous violation of supersymmetry happens when F gains a vacuum expection value. As follows from the Goldstone theorem, a massless particle appears in the spectrum that is a fermion, the goldstino. It becomes a longitudinal component of the gravitino in supergravity, such that ψ — goldstino $\stackrel{SUGRA}{\longrightarrow}$ longitudinal gravitino, where supersymmetry is promoted to a local symmetry.

Goldstino superpartners are

$(\varphi + \varphi^*) \to S$ — scalar sgoldstino
$(\varphi - \varphi^*) \to P$ — pseudoscalar sgoldstino

These particles are

- massless at tree level, but become massive due to high order corrections.
- R-even like SM particles, which thus allows single sgoldstino production by SM particles, and decay into SM particles (see the effective Lagrangian in [5, 6]),
- and candidates to explain the HyperCP anomaly in $\Sigma \to p\mu^+\mu^-$ [7] as production of pseudoscalar sgoldstino [8] of $m_P = 214.3$ MeV.

Given the sgoldstino mass scale and coupling pattern, their signatures at e^+e^--colliders [9, 10], at the TeVatron [11, 12], and at the LHC [13, 14, 15] have been extensively investigated.

Sgoldstinos are naturally light in no-scale SUGRA [16, 17] and in models with gauge mediation mechanism of SUSY breaking [18, 19]. The sgoldstino interaction terms are proportional to the ratio of the soft mass terms and the SUSY breaking parameter: $\mathcal{L}_{S,P} \propto \frac{M_{\rm superpartners}}{F}$ with an order-of-magnitude estimate of $F \sim (\text{SUSY breaking scale})^2$.

With the coupling to gluons being the strongest, the sgoldstino decay rate is naturally dominated by decays to pions. Decays into lepton pairs and photon pairs are subdominant, though the decay pattern may be different for different patterns of the soft SUSY breaking terms. For the sgoldstino lifetime one obtains

$$\tau_X = 10^{-6}\,\mathrm{s}\,\times\left(\frac{\sqrt{F}}{1000\,\mathrm{TeV}}\right)^4\left(\frac{3\,\mathrm{TeV}}{M_{\lambda_g}}\right)^2\left(\frac{1\,\mathrm{GeV}}{m_X}\right)^3$$

where M_{λ_g} refers to gluino mass. Hence, at fixed target experiments the sgoldstinos are produced in D-meson decays with lifetimes which allow them to travel $O(km)$. They subsequently decay into [2]

$$X \to \pi^+\pi^-\,,\quad \pi^0\pi^0\,,\quad \mu^+\mu^-\,,\quad e^+e^-\,,\quad \gamma\gamma$$

To estimate the sensitivity of the proposed experiment to for instance a light *scalar* sgoldstino one can follow the steps adopted in searches for the light Higgs boson [20] or other light singlet scalars, see e.g. [21]. In the case that the coupling to gluons dominate both production and decays, and 2×10^{20} pots, the expected number of signal $\pi^+\pi^-$ pairs in the proposed experiment may be written as

$$N_{\pi^+\pi^-} \simeq 2 \times \left(\frac{1000\,\mathrm{TeV}}{\sqrt{F}}\right)^8\left(\frac{M_{\lambda_g}}{3\,\mathrm{TeV}}\right)^4\left(\frac{m_X}{1\,\mathrm{GeV}}\right)^2$$

2.2.2 R-parity violating neutralinos in SUSY

Motivated by the stability of the proton one can introduce R-parity in supersymmetric extensions of the SM so that all the superpartners are R-odd, while the SM particles (and additional Higgs bosons) are R-even. As a results, the lightest superpartner, LSP, is stable and hence constitute a candidate for Dark Matter.

If R-parity is (slightly) broken (it may be done while keeping proton long-lived enough, see e.g. [22] for details and theoretical motivations), the LSP becomes unstable. However, cosmological considerations still imposes constraints since it requires that [23]

- if the LSP is long-lived, then
$$\tau_{\mathrm{LSP}} > 10^{18}\,\mathrm{yr}$$
to suppress the contribution of the LSP decay products in the galactic cosmic rays (e.g. to the γ-background measured by FERMI)

- if the LSP is short-lived, then
$$\tau_{\mathrm{LSP}} < 0.1\,\mathrm{s}$$
to decay before the Big Bang Nucleosynthesis so that the highly energetic SM particles from the LSP decays get thermalized in the primordial plasma and do not spoil the subsequent production of light nuclei and their relative abundance.

Direct searches at the LHC (and previously at the Tevatron) are quite a challenge if the LSP decays outside the detectors of ATLAS and CMS (CDF and D0), see e.g. [24]. Clearly, fixed target experiments with remote detectors may probe significantly longer lifetimes than collider experiments [3].

At a fixed target experiment, the light neutralinos χ_0 would be produced mostly in pairs through the decays of heavy hadrons via R-conserving couplings [25]

$$B \to K\chi_0\chi_0$$

which is the process probed by Belle [26], or via R-violating couplings [3]

$$B^{\pm} \to l^{\pm}\chi_0\,, \quad \text{and} \quad B^0 \to \nu\chi_0$$

which are the processes probed by BaBar [27, 28] and Belle [29]. The long lifetimes allow the light neutralino to travel a significant distance before decaying into SM particles. It might be responsible [30, 3] for the NuTeV dimuon events [31] through the decay mode

$$\tilde{\chi}_0 \to \mu^+\mu^-\nu \tag{1}$$

See also further searches reported in [32].

The proposed experiment would achieve a significantly higher sensitivity by exploiting the analogous decay modes of charmed mesons with neutralinos in the final states. With 2×10^{20} pots the expected number of signal events in the proposed detector of the type in (1) may be written as

$$N \simeq 20 \times \left(\frac{m_{\chi_0}}{1\,\mathrm{GeV}}\right)^6 \left(\frac{\lambda}{10^{-8}}\right)^2 \left(\frac{\mathrm{Br}\,(D \to \chi_0 + \ldots)}{10^{-10}}\right)$$

where the R-violating coupling λ governs the neutralino decays. Their rates are proportional [3] to $\Gamma \propto \lambda^2 m_{\chi_0}^5$.

2.2.3 Massive vectors (paraphotons)

The vector portal naturally arises in the framework of the Mirror World, see [33] for a review. It may provide a coupling to the mirror matter, including that which plays the role of Dark Matter (e.g. mirror baryons). Generally, the vector portal to the secluded sector may couple to e.g. WIMP-like Dark Matter Ψ, $\bar{\Psi}$ [4].

Having one more $U'(1)$ gauge group (this time in a secluded sector) naturally implies mixing with our $U_Y(1)$, see e.g. [34],

$$\frac{\epsilon}{2} F'_{\mu\nu} F_{\mu\nu}$$

This coupling is renormalizable and ϵ is dimensionless. Hence it is unsuppressed at any (high) energy scale. If the new $U'(1)$ gauge group is spontaneously broken by a Higgs mechanism operating in the secluded sector, the vector field becomes massive.

The massive (para)photon can be light, e.g. $m_{\gamma'} \sim 1\,\mathrm{GeV}$, and hence may be produced in fixed target experiments through a virtual photon, $\sigma \propto \epsilon^2$. The subsequent decay is again through a virtual photon, $\Gamma \propto \epsilon^2$, into pairs of the kinematically allowed SM electrically charged particles,

$$\gamma' \to e^+e^- \,,\; \mu^+\mu^- \,, \ldots$$

Cosmology provides lower limits on ϵ:

- Big Bang Nucleosynthesis:

$$\tau_{\gamma'} < 0.1\,\mathrm{s} \quad \Longrightarrow \epsilon^2 \left(\frac{m_{\gamma'}}{1\,\mathrm{GeV}}\right) \gtrsim 10^{-21}$$

- Ψ as WIMP-like Dark Matter requires it to be thermalized in the primordial plasma of SM particles at an early stage in the expansion of the Universe:

$$\epsilon^2 \left(\frac{m_{\gamma'}}{1\,\mathrm{GeV}}\right) \gtrsim 10^{-11} \times \left(\frac{m_\Psi}{500\,\mathrm{GeV}}\right)^2$$

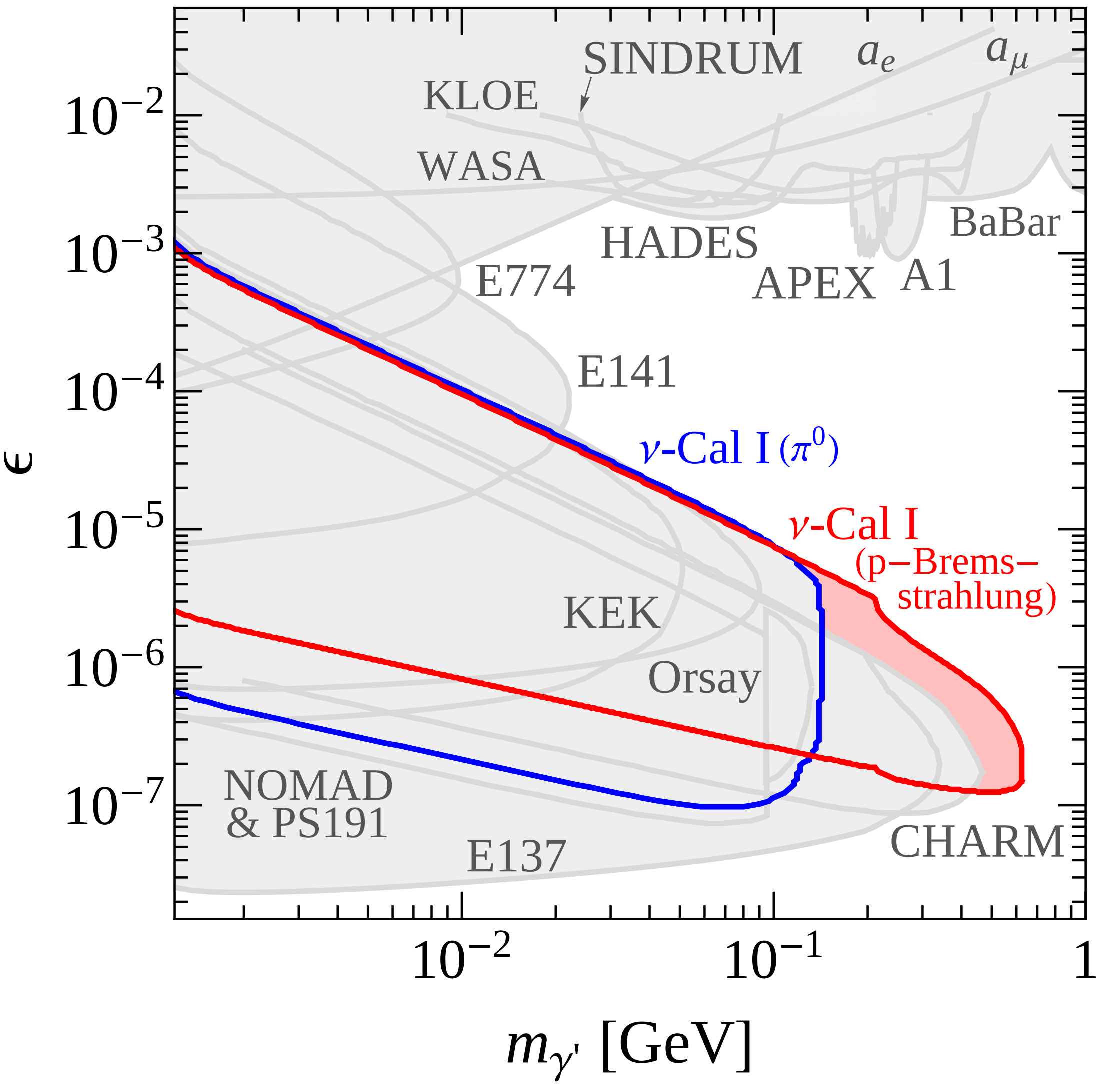

Figure 1: Present direct limits on the model parameter space (ϵ,$m_{\gamma'}$), for details and original references see [36].

The present direct limits (for a recent brief review see [35]) on the model parameter space $(\epsilon, m_{\gamma'})$ are presented in Fig. 1, see also [35].

The paraphoton production rate at a fixed target experiment with a proton beam has been estimated in [36] for proton Bremsstrahlung, see also [37] for contribution of η- and η'-mesons. From this it is expected that the proposed experiment is able to improve the CHARM limits on ϵ for the interesting mass range by at least two orders of magnitude. Note that the recently submitted proposal to the SPSC to search for paraphotons with an electron beam dump [38] is sensitive to lighter paraphotons with larger mixing ϵ.

3 Q2: Beyond the test of the νMSM does the EoI address a broader class of extensions of the Standard Model including heavy neutral leptons ? If yes, which other models would be tested by the current EoI ?

3.1 Survey of HNL models

The models with HNLs with masses from 100 MeV to 2 GeV have a long history, which may be found in the references of the EOI of the proposed experiment. More recently, they were studied in a number of popular BSM setups:

- Type-I seesaw in models with dynamical electroweak symmetry breaking (extended technicolor) [39, 40, 41]
- Low scale gauged $U(1)_{B-L}$ extension of the Standard Model [42]
- In extended double seesaw model (neutrino masses and low scale leptogenesis) [43]
- Five-dimensional Randall-Sundrum-like models (mini-seesaw mechanism in warped space) [44, 45]
- Classically conformal Standard Model with the Higgs portal [46]
- Symmetries behind νMSM-like spectrum of masses [47, 48, 49]

3.2 Hierarchy of models with HNL

From a phenomenological point of view, the models with HNLs can be divided into the following categories:

- (i) the νMSM: HNLs are required to explain neutrino masses, baryon asymmetry, and Dark Matter
- (ii) HNLs are required to explain neutrino masses and baryon asymmetry
- (iii) HNLs are required to explain neutrino masses
- (iv) HNLs are required to explain Dark Matter
- (v) HNLs are helpful in cosmology and astrophysics

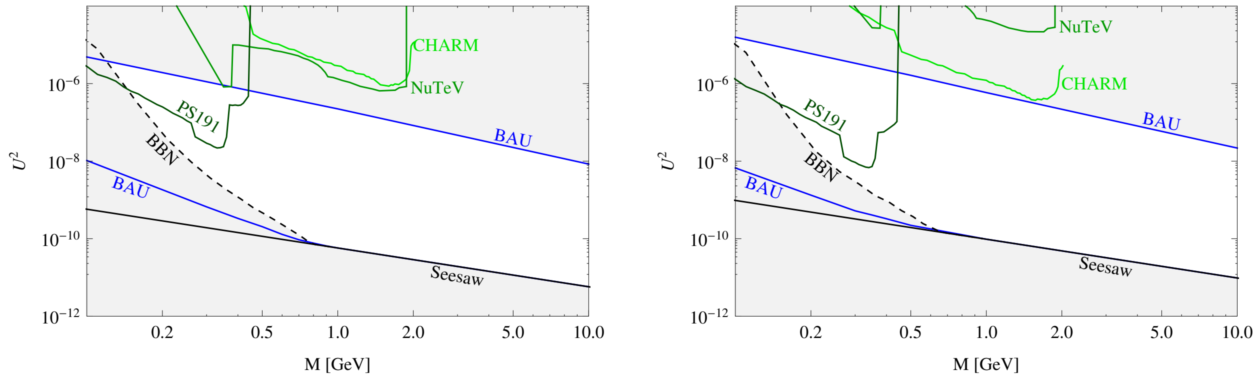

Figure 2: Current bounds in the νMSM on the parameters of the degenerate HNLs, $N_{2,3}$ in the (U^2, M_N) plane from cosmological considerations and neutrino mixing together with limits from previous experimental searches (the solid and dashed lines indicate the dependence of these regions on the pattern of HNL mixing with the electron, muon and tau-neutrino). Figures taken from Ref. [50]. A normal mass hierarchy of the neutrinos is shown on the left and an inverted hierarchy on the right.

- (vi) HNLs are not required to explain anything - just so

The constraints on the properties of HNLs in the different categories are reviewed shortly below.

3.2.1 (i) The νMSM

The constraints on the mixing angle U^2 are the most strongest if we want to explain neutrino masses, baryon asymmetry, and Dark Matter simultaneously. The lightest HNL N_1 - DM candidate - almost decouples, so that only the two particles N_2 and N_3 remain to make the Universe asymmetric and the neutrinos massive. It follows that N_2 and N_3 must be nearly degenerate. The challenging aim of the current proposal is to explore the cosmologically interesting region of the parameter space of the νMSM, shown in Fig. 2.

3.2.2 (ii) HNLs to explain neutrino masses and baryon asymmetry

If the Dark Matter particle is not a HNL but something else (axion, WIMP or other exotics), then all three N can participate in the see-saw formula to generate the active neutrino masses and in baryogenesis. In comparison with the previous case there is more freedom, and the constraints on the mixing angle U^2 are considerably more relaxed. The most important consequences [51] are:

- Degeneracy between N's is not needed anymore. Since $M \ll T_{\rm sph} \sim 150$ GeV, the energies of N's with the same momenta are very close to each other, and resonant oscillations of N's occur, leading to leptogenesis and baryogenesis. Here $T_{\rm sph}$ is the sphaleron freeze-out temperature, after which the conversion of lepton number to baryon number switches off.

- Generation dependent mixing angles U_μ^2, U_τ^2 can be much larger than previously, allowing the leptonic μ and τ flavours to equilibrate, while the Sakharov non-equilibrium condition is satisfied only for the electronic flavour to make baryogenesis possible. Successful baryogenesis may take place even with $U_\mu^2 \sim 10^{-3}$.

3.2.3 (iii) HNLs to explain neutrino masses

If HNLs are not required to produce the baryon asymmetry of the Universe (it can arise, for example, in the electroweak phase transition or due to some other mechanism, for a review see [52]), nor contribute to Dark Matter, the constraints on their properties are even weaker.

The only source of information on the mixing angles U come from the see-saw formula, and from the only partially known active neutrino mixing matrix:

$$[m_\nu]_{\alpha\beta} = -[M_D]_{\alpha I} \frac{1}{M_I} [M_D]_{\beta I} \ . \tag{2}$$

Here $[M_D]_{\alpha I}$ are the Dirac masses of the active neutrinos, and M_I are the Majorana masses of the HNLs. The mixing angles U^2 can be as large as ~ 1, so that only the direct experimental constraints on U^2 remain. As was argued in our EOI, these can be improved considerably with the proposed experiment.

At the same time, as shown in [53], the *lower bound* on the relevant mixing angles U_e^2, U_μ^2 still exists, see Fig. 3. They can be used for fixing the ultimate goal of the fixed target experiment.

3.2.4 (iv) HNLs to explain Dark Matter

A HNL with a mass in the keV region is an excellent Dark Matter candidate [54, 55, 56, 57]. The lifetime of these particles greatly exceeds the age of the Universe (see Fig. 4, left panel), and their mixing angle is quite small, see Fig. 4, right panel.

These particles cannot be found in fixed target experiments. Their search requires high resolution X-ray telescopes in space [57, 58, 59].

3.2.5 (v) HNLs in cosmology and astrophysics

The role of HNLs in cosmology and astrophysics has been investigated in a number of works. Several examples are given below:

- HNLs may influence the primordial abundance of light elements and the effective number of relativistic degrees of freedom [60, 61, 62, 63, 64, 65, 66]

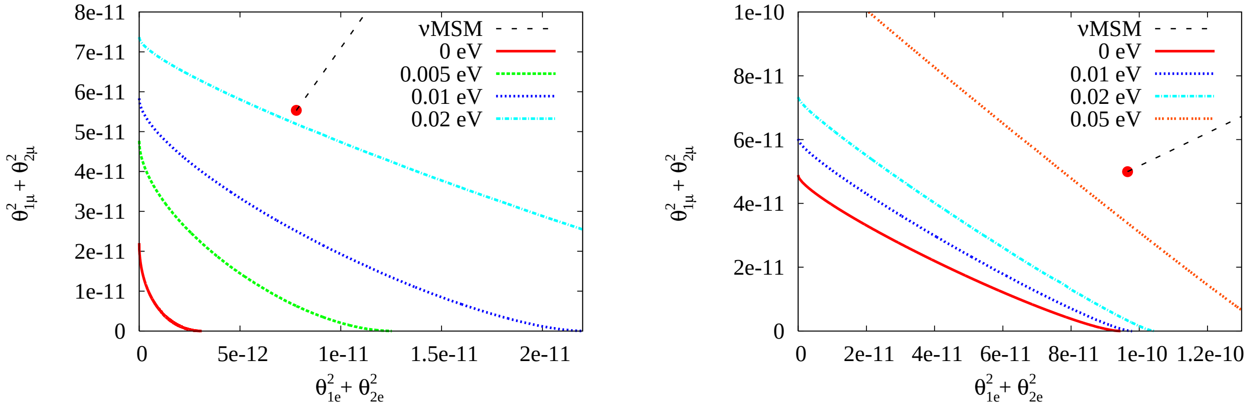

Figure 3: The minimal values of mixings for $M_1 = M_2 = 500$ MeV and: (a) normal hierarchy, (b) inverted hierarchy of active neutrino masses. The different lines correspond to different values of the lightest active neutrino mass m_{lightest}. On both plots the dashed line refers to the mixing in the νMSM.

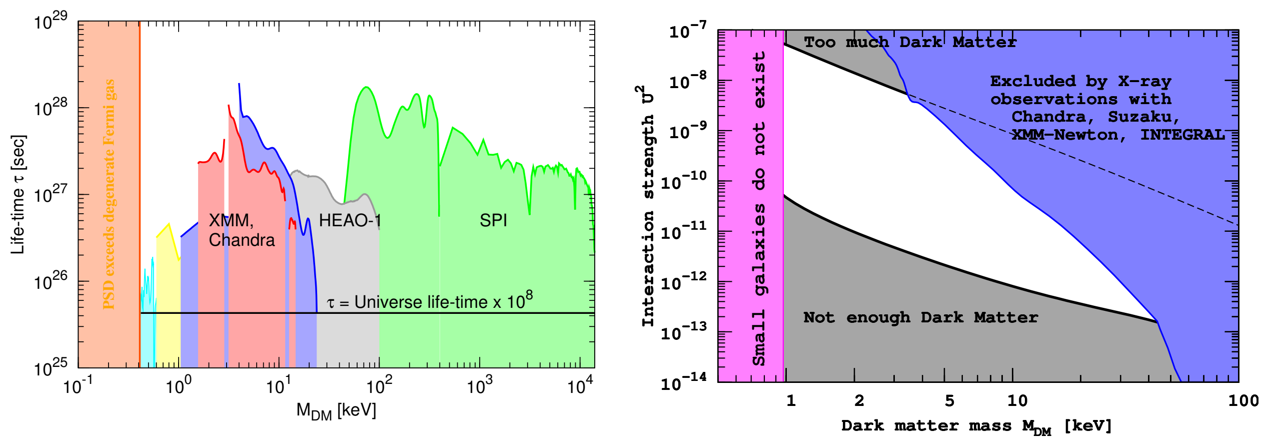

Figure 4: The observational bounds on the properties of HNLs that play the role of Dark Matter particles. Left: lower bounds on the lifetime of HNLs from X-ray observations compared with the lifetime of the Universe (the horizontal black line). Right: bounds on the mixings of HNLs from X-ray observations (upper bound, blue shaded region), and from the requirement that *all* the Dark Matter in the Universe is composed of the HNLs (upper and lower bounds, grey shaded regions). On both plots, the region of masses of HNLs below ~ 1 keV is excluded from the phase-space density constraints, and the blank regions correspond to the *allowed* parameter space.

- HNLs are used in low reheating models, in which the temperature of the Universe never exceeded a few MeV and is coming from HNL decays [67]

- Entropy production from HNL decays [68] to reduce the abundance of unwanted relics

- HNLs with masses below 250 MeV can facilitate the explosions of supernovae [61, 69], as they provide a new channel of energy transfer from the inner to the outer regions.

3.2.6 (vi) Just so HNLs

The phenomenology of "just so" HNLs was considered in many works. Clearly, in this case only experimental constraints on their masses and mixing angles exist. The HNLs can lead to a number of interesting processes which may be accessible in both collider and in fixed target experiments:

- Contributions of the HNLs to the rare lepton number violating processes $\mu \to e\gamma$ and $\mu \to eee$ [70]
- Contribution to the neutrinoless double beta decay [71, 72, 73, 74]
- Prospects for searches for νMSM-like HNLs with LBNE experiment are discussed in [75]
- Ref. [76] discusses bounds on the mixing of HNLs with τ-neutrinos
- Refs. [77, 78] discuss strategies for searching HNLs in the decays of π and K mesons
- Ref. [79] discusses collider signatures of sterile neutrinos with mass > 1 GeV, where they acquire a mass via a coupling to an additional singlet Higgs field;
- Experimental bounds on the mixing $U^2_{e,\mu}$ and their combination from analysis of the bounds on lepton number and lepton flavour number violating decays of τ-leptons and B, D, K-mesons [80].
- Searches for sterile neutrinos in the data of the E949 experiment at BNL for masses between M_π and M_K are discussed in [81]
- In the Ref. [82] bounds in the range $1 - 13$ GeV were obtained under the assumption that sterile neutrinos are produced by some other mechanism, not suppressed by U^2.
- The branching ratios of decays of heavy mesons and baryons with sterile neutrinos in the final states as well as the subsequent decays of sterile neutrinos to Standard Model particles has been discussed in [83, 84, 80, 85, 86]
- [87] summarizes past and discusses future accelerator searches in the mass range $8 - 390$ MeV;
- Peak searches: [88],[89] $50 - 130$ MeV; [90] $70 - 300$ MeV; proposals: [81] $140 - 500$ MeV

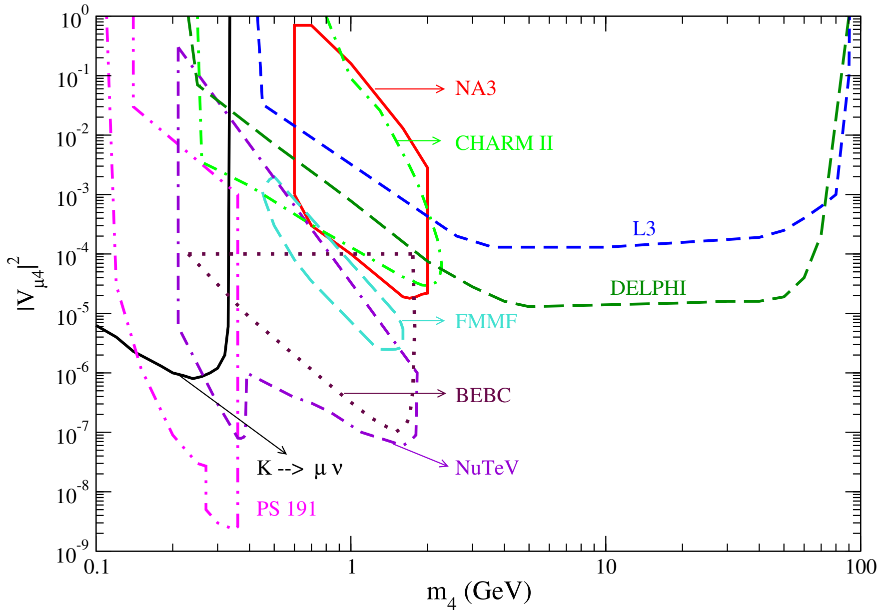

Figure 5: Current experimental upper bounds on the mixing of the HNLs with the muon neutrino. The area with the solid black contour labeled $K \to \mu\nu$ [87] is excluded by peak searches. The other bounds indicated by contours labeled by PS191 [92], NA3 [101], BEBC [102], FMMF [103], NuTeV [93] and CHARMII [104] correspond to the beam-dump experiments with limits at 90% C.L., while DELPHI [105] and L3 [106] correspond to collider experiments at LEP with limits at 95% C.L. The figure is taken from Ref. [100].

- Fixed target searches: [91],[92] $\leq 450\,\mathrm{MeV}$; [93] - $250\,\mathrm{MeV} - 200\,\mathrm{GeV}$; [94] $0.5 - 2.8\,\mathrm{GeV}$; [95] $10 - 190$ MeV

  The original ideas of peak searches: [96, 97, 98, 99]

The summary of HNL searches [100] is shown in Fig. 5.

In addition, the search for HNLs in B-decays was recently reported by Belle Collaboration [107].

4 Q3: The experimental sensitivity should be assessed through more precise simulations, including systematics, backgrounds, efficiencies and other production/decay channels.

At this stage we do not have a full Geant description of our apparatus. We use Pythia and Geant scoring planes to check acceptances, but there is no reconstruction of tracks/showers. However, the detection efficiency in the HNL search is entirely dominated by the limited geometrical acceptance with respect to the long HNL lifetime, and this has been properly taken into account. For instance at a typical lifetime of 1.8×10^{-5}s, the geometrical acceptance is about 8×10^{-5}. As a result, reconstruction effects are not expected to change significantly the experimental sensitivity.

4.1 Sensitivity to the HNL decay channels with neutrals and electrons in the final state

As mentioned in Section 2.2 of the EOI, the most promising decay channel is $N \to \mu^- \pi^+$ since it provides the cleanest signature. It is planned that the spectrometer contains an electromagnetic calorimeter, which allows extending the search to include $N \to e\pi$ and $N \to \mu\rho^{\pm}(\to \pi^{\pm}\pi^0)$. Fig. 6 shows the energy spectrum of the electrons from $N \to e^-\pi^+$ decays at the front of the electromagnetic calorimeters. More than 99 % of the electrons have sufficient energy to be distinguished from MIPs.

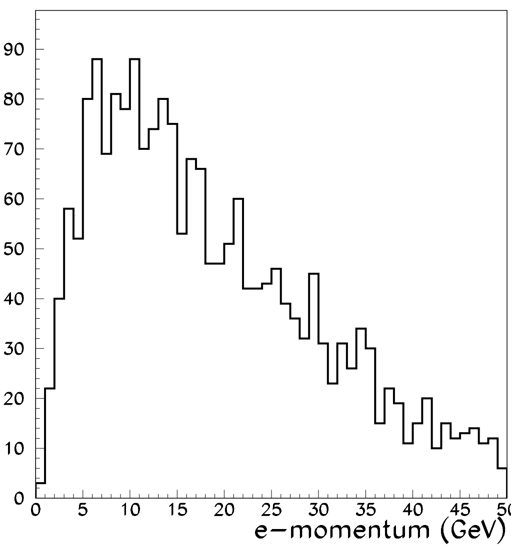

Figure 6: The energy of electrons from $N \to e^-\pi^+$ decays within the acceptance of the electromagnetic calorimeter.

Fig. 7 show the energy and topology of the photons from the π^0-decay in $N \to \mu\rho^{\pm}(\to \pi^{\pm}\pi^0)$ decays at the electromagnetic calorimeters. While most photons have sufficient energy to distinguish them from MIPs, it is clear that the π^0 detection efficiency may be improved with a cell size of $< 10 \times 10$ cm^2 in order to resolve the photons. In addition the distance between photons does not show a strong dependence on their position, and hence a small cell-size is required for the whole calorimeter.

Fig. 8 shows a comparison of the fraction of HNL decays which can be reconstructed in the spectrometer as a function of the length of the muon filter. This assumes an electromagnetic

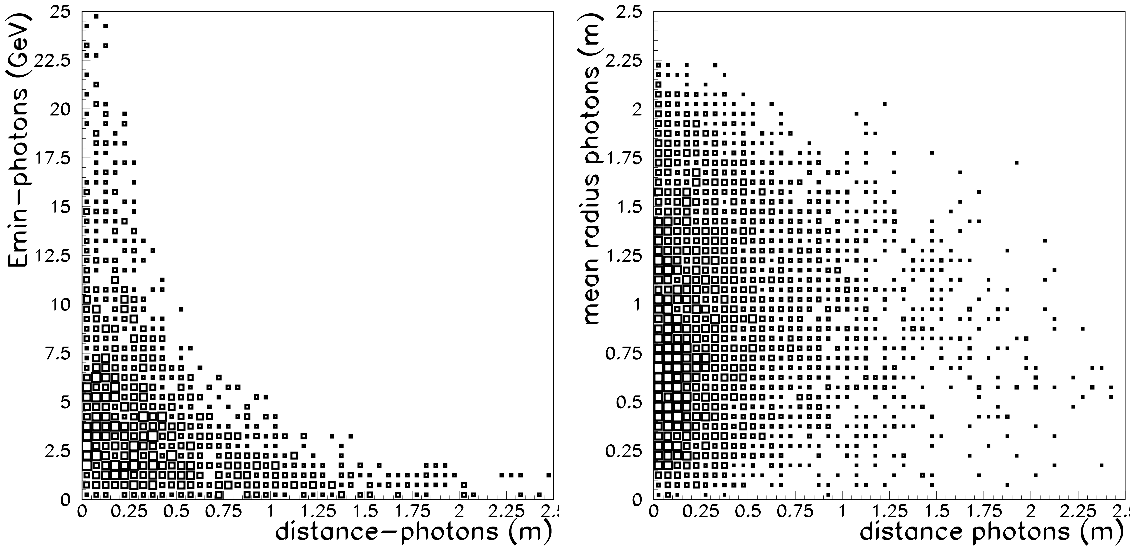

Figure 7: The energy and topology of photons from π^0-decay in $N \to \mu\rho^{\pm}(\to \pi^{\pm}\pi^0)$ decays.

calorimeter with a cells-size of 10×10 cm^2, and requires $E_{e(\gamma)} > 1.(0.5)$ GeV, and for the π^0 reconstruction at least 20 cm between the two photons. It shows that the electromagnetic calorimeter will allow detection of $N \to e^-\pi^+$ with a similar efficiency to that of $N \to \mu^-\pi^+$. It will also enable the detection of $N \to \mu\rho^{\pm}(\to \pi^{\pm}\pi^0)$ decays, albeit with a $\sim$ 45 % reconstruction efficiency compared to $\mu\pi$. Fig. 8 also shows that a small change in the length of the muon filter does not result in a large effect on the acceptance.

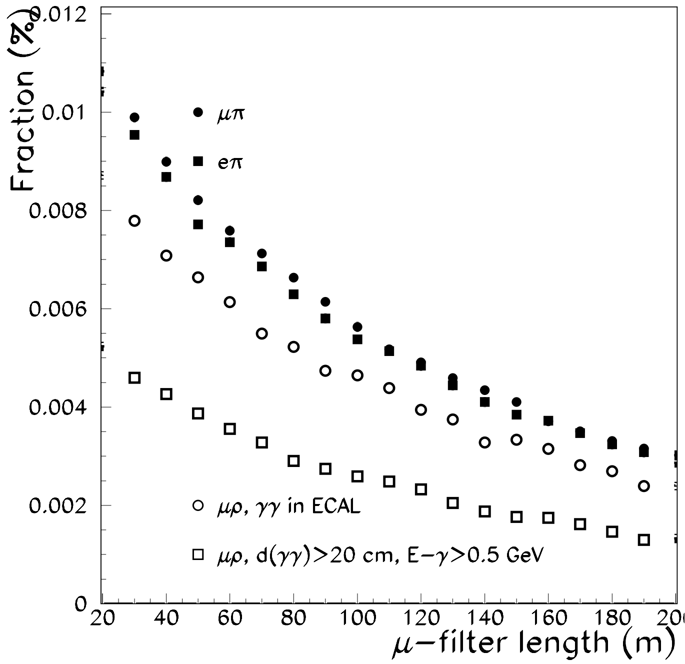

Figure 8: Comparison of the fraction of reconstructed N decays assuming $\tau_{\mathrm{HNL}} = 1.8 \times 10^{-5}$ s and $M(N) = 1$ GeV.

5 Q4:What is the expected transverse size of the muon absorber ? Q5: It was suggested that a magnetized muon absorber could be shorter and therefore more affordable. Did you consider this option ? Q6: As the hadron and muon filters are likely to be one of the cost drivers of the project, it would be important to define the choice of material and dimensions of the muon filter. The choice between uranium or tungsten should include the safety and legal implications in the case of uranium.

The active and passive muon shield options are being studied with Geant4 simulations. A status report (see slides of T. Ruf https://indico.cern.ch/conferenceDisplay.py?confId=287749) has been presented to the referees at the meeting on December 11. The aim is to continue this study and perform further optimization. Here we present a brief summary of our preliminary conclusions.

In order to reduce the muon induced background to a level comparable to the background induced by the active neutrinos, the shielding should reduce the rate of muons leaving the target and the hadron absorber and reaching the detector volume from 5×10^9 to less than 10×10^3 per spill. The initial muon flux is based on spills of 5×10^{13} pot in order to take a conservative approach.

For the active shielding, conventional iron magnets operated at low power with a field of 1.85T seem to be the best option. Given the transverse detector radius of about 2.5m and its distance from the proton target of 100m, an integral field of about 40Tm is needed to deflect muons of up to 400GeV/c momenta. The alternative of high field magnets (3T) with an air gap to minimize multiple scattering, as in the DONUT experiment, is disfavoured. The much larger air gap required in the proposed experiment due to the angular spread of the muons from the proton interactions in the target and due to the distance of 3.5m to the entrance of the magnet, leads to a large power consumption.

The simulations show that, due to the return field and the multiple scattering in the magnet material, an active shielding alone is not sufficient. An additional passive shielding made of iron is necessary to stop the low momentum muons entering the detector region. As shown in the attached report, in this way a residual muon rate of 40×10^3 / spill is obtained. Further optimization of the return field and the passive shielding is required. For this purpose an event display was developed (see Fig. 9). It already allowed identifying several improvements in the layout and it seems possible to reduce the rate to $\approx 3 \times 10^3$ / spill.

A potential serious drawback of the active shielding is the high flux of muons travelling through the iron shield. Geometrically it is not oriented towards the detector planes, but it produces long-lived particles in the last interaction length which may reach into the detector decay volume. More simulations are required to establish the impact.

For the passive shielding, the use of a tungsten cone of about 250t together with additional lead shielding (2100t) and a total length of the passive shielding of 70m reduces the rate down to 3.5×10^3 / spill. With a smaller tungsten cone of 86t and more lead, the rate increases to 20×10^3 / spill. The corresponding loss of acceptance of about 15% (see Fig. 8), by moving the detector further downstream seems acceptable.

In summary, both options, active+passive and solely passive shielding are viable options. However, the solely passive shielding seems more robust against uncertainties in the details of the simulation.

More optimizations are needed to further reduce the rates and the material. In particular, the effect of the muon interactions in the material close to the decay volume needs to be

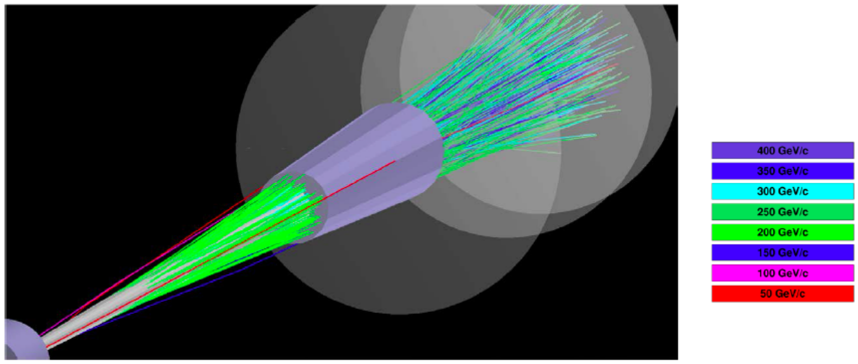

Figure 9: Event display for the muon shield simulations.

studied.

For the question of using tungsten or alternatively uranium, uranium has not been seriously considered at this stage. In terms of performance for ranging out muons, the two materials are very similar. Should uranium be available or turn out to be cheaper in acquisition, it appears plausible that the security and the safety aspects may be respected by its isolated location in the shielding tunnel. It should also be possible to respect the radiological aspects. The hadron absorber should provide sufficient shielding to prevent exposition of the uranium to direct radiation. However, this may only be ensured by accurate simulation. Moreover, the radioactivation by the muon flux must be properly evaluated.

6 Q7: In your comparison with other facilities (Section 6.1 of the EoI) you did not consider the case of a high energy proton beam at FNAL tuned at 400 GeV and with the intensity boosted by Project X. Is this excluded?

At present, the FNAL Main Injector has 400 kW of protons at 120 GeV (2.1×10^{13} pot/s), to be compared to the 500 kW of protons at 400 GeV at the SPS (7.8×10^{12} pot/s). Next year, the Main Injector will undergo an upgrade (PIP) to 700 kW (always at 120 GeV, that is 3.6×10^{13} pot/s).

Project X was intended to provide a 2.4 MW proton beam at a maximum energy of 120 GeV (1.2×10^{14} pot/s). However, the project was recently downscoped (though not yet officially approved) to a new project called PIP-II (http://www.fnal.gov/pub/today/archive/archive_2013/today13-12-13.html), and (https://indico.bnl.gov/getFile.py/access?contribId

=11&sessionId=5&resId=0&materialId=slides&confId=680), which has a lower beam intensity projected, i.e. 1.2 MW at the startup in 2025 and >2 MW in the long term (>2030) with the 120 GeV beam aiming at the long baseline neutrino oscillation experiment LBNE. For the startup phase the expected spill intensity is 7.5×10^{13} every 1.2s. While we did not perform a thorough simulation with a 120 GeV beam, we can make the following considerations. At 120 GeV the charm production cross-section is only about 10% of that at 400 GeV. The acceptance for the HNL at a given distance from the target would be lower due to the lower boost and the consequently wider angular distribution. On the other hand, the minimum bias cross-section is only 75% lower at 120 GeV, suggesting that the beam backgrounds do not scale in the same way as the signal. In addition, the pions and kaons are produced at a lower boost, suggesting that a larger fraction decays before being stopped in the target, hence leading to a further increase of the relative muon flux. Therefore, it is expected that the muon dump would be only marginally shorter at 120GeV.

7 Q8: Can you quote an order of magnitude of the cost of the various parts of the experiment (beam, detector, infrastructure, etc.) ?

Figure 10 shows a very preliminary cost estimate. The cost of the civil engineering and the beam line is obviously site specific. The current cost estimate has been prepared by using information from existing and projected facilities, and in consultation with experts. At this stage the cost does not assume reuse of any facility or any equipment. All civil engineering assumes conservatively the use of diaphragm walls along the entire length of the construction.

The HNL detector is entirely based on existing technologies. The experience with these technologies is fully covered by the various groups who have expressed interest in participating to the experiment. This should also allow reducing the cost.

8 Q9: What are the prospects of the Collaboration to extend beyond the list of proponents ?

Below is a list of seminars and conference talks which have been either given or committed by the proponents since the presentation of the EoI at the SPSC open session on October 23, 2013

Seminars:

Civil engineering primary beam line	40
Civil engineering target facility	
Civil engineering muon shield tunnel	
Civil engineering detector facility	
Facility infrastructure	
Primary beam line extension and delivery	20
Target station and hadron absorber	10
Muon shield	20
Pre-study, design, engineering, tendering (10%)	10
2 x Detector element	30
Online system + computing	2
Total	132

Figure 10: Preliminary cost estimate in MCHF

- Imperial College (London), University of Oxford, University of Liverpool, University of Manchester, Rutherford Appleton Laboratory
- ITEP (Moscow), JINR (Dubna), INR(Moscow)
- IRFU/SPP CEA Saclay
- Instituto de Fisica da USP (Sao Paulo), UFRJ (Rio de Janeiro)
- NIKHEF (Amsterdam)
- University of Munich
- University of Bern
- Kavli Institute (Tokyo)
- University of Melbourne, University of Sydney
- Universidad Tcnica Federico Santa Mara (Valparaiso)
- University of Stockholm, University of Uppsala

Conference talks:

- UK HEP Forum, November 2013
- High Energy Physics in the LHC Era, Valparaiso, Chile, 16-20 December 2013
- ICFA Neutrino European meeting, Paris, 8-10 January 2014

In addition we have had working meetings with the groups from University of Bern (Switzerland) and University of Napoli (Italy)

References

[1] B. Batell, M. Pospelov and A. Ritz, *Exploring Portals to a Hidden Sector Through Fixed Targets*, *Phys.Rev.* **D80** (2009) 095024 [0906.5614].

[2] D. Gorbunov, *Light sgoldstino: Precision measurements versus collider searches*, *Nucl.Phys.* **B602** (2001) 213–237 [hep-ph/0007325].

[3] A. Dedes, H. K. Dreiner and P. Richardson, *Attempts at explaining the NuTeV observation of dimuon events*, *Phys.Rev.* **D65** (2001) 015001 [hep-ph/0106199].

[4] M. Pospelov, A. Ritz and M. B. Voloshin, *Secluded WIMP Dark Matter*, *Phys.Lett.* **B662** (2008) 53–61 [0711.4866].

[5] A. Brignole, F. Feruglio and F. Zwirner, *Aspects of spontaneously broken N=1 global supersymmetry in the presence of gauge interactions*, *Nucl.Phys.* **B501** (1997) 332–374 [hep-ph/9703286].

[6] D. S. Gorbunov and A. V. Semenov, *CompHEP package with light gravitino and sgoldstinos*, hep-ph/0111291.

[7] **HyperCP** Collaboration, H. Park *et. al.*, *Evidence for the decay* $\Sigma^+ \to p\mu^+\mu^-$, *Phys.Rev.Lett.* **94** (2005) 021801 [hep-ex/0501014].

[8] D. Gorbunov and V. Rubakov, *On sgoldstino interpretation of HyperCP events*, *Phys.Rev.* **D73** (2006) 035002 [hep-ph/0509147].

[9] D. A. Dicus, S. Nandi and J. Woodside, *Unusual* Z^0 *decays in supersymmetry with a superlight gravitino*, *Phys.Rev.* **D43** (1991) 2951–2955.

[10] E. Perazzi, G. Ridolfi and F. Zwirner, *Signatures of massive sgoldstinos at e+ e- colliders*, *Nucl.Phys.* **B574** (2000) 3–22 [hep-ph/0001025].

[11] D. A. Dicus and S. Nandi, *New collider bound on light gravitino mass*, *Phys.Rev.* **D56** (1997) 4166–4169 [hep-ph/9611312].

[12] E. Perazzi, G. Ridolfi and F. Zwirner, *Signatures of massive sgoldstinos at hadron colliders*, *Nucl.Phys.* **B590** (2000) 287–305 [hep-ph/0005076].

[13] D. Gorbunov, V. Ilyin and B. Mele, *Sgoldstino events in top decays at LHC*, *Phys.Lett.* **B502** (2001) 181–188 [hep-ph/0012150].

[14] D. Gorbunov and N. Krasnikov, *Prospects for sgoldstino search at the LHC*, *JHEP* **0207** (2002) 043 [hep-ph/0203078].

[15] S. Demidov and D. Gorbunov, *LHC prospects in searches for neutral scalars in $pp \to \gamma\gamma + jet$: SM Higgs boson, radion, sgoldstino*, *Phys.Atom.Nucl.* **69** (2006) 712–720 [hep-ph/0405213].

[16] J. R. Ellis, K. Enqvist and D. V. Nanopoulos, *A Very Light Gravitino in a No Scale Model*, *Phys.Lett.* **B147** (1984) 99.

[17] J. R. Ellis, K. Enqvist and D. V. Nanopoulos, *NONCOMPACT SUPERGRAVITY SOLVES PROBLEMS*, *Phys.Lett.* **B151** (1985) 357.

[18] G. Giudice and R. Rattazzi, *Theories with gauge mediated supersymmetry breaking*, *Phys.Rept.* **322** (1999) 419–499 [hep-ph/9801271].

[19] S. Dubovsky, D. Gorbunov and S. V. Troitsky, *Gauge mechanism of mediation of supersymmetry breaking*, *Phys.Usp.* **42** (1999) 623–651 [hep-ph/9905466].

[20] J. R. Ellis, M. K. Gaillard and D. V. Nanopoulos, *A Phenomenological Profile of the Higgs Boson*, *Nucl.Phys.* **B106** (1976) 292.

[21] F. Bezrukov and D. Gorbunov, *Light inflaton Hunter's Guide*, *JHEP* **1005** (2010) 010 [0912.0390].

[22] H. K. Dreiner, *An Introduction to explicit R-parity violation*, hep-ph/9707435.

[23] J. R. Ellis, G. Gelmini, J. L. Lopez, D. V. Nanopoulos and S. Sarkar, *Astrophysical constraints on massive unstable neutral relic particles*, *Nucl.Phys.* **B373** (1992) 399–437.

[24] T. Adams, *Searches for Long-lived Particles at the Tevatron Collider*, *Mod.Phys.Lett.* **A23** (2008) 371–385 [0802.1048].

[25] H. Dreiner, S. Grab, D. Koschade, M. Kramer, B. O'Leary *et. al.*, *Rare meson decays into very light neutralinos*, *Phys.Rev.* **D80** (2009) 035018 [0905.2051].

[26] **Belle** Collaboration, O. Lutz *et. al.*, *Search for $B \to h^{(*)}\nu\bar{\nu}$ with the full Belle Y(4S) data sample*, *Phys.Rev.* **D87** (2013) 111103 [1303.3719].

[27] **BaBar** Collaboration, B. Aubert *et. al.*, *Search for B^0 decays to invisible final states and to $\nu\bar{\nu}\gamma$*, *Phys.Rev.Lett.* **93** (2004) 091802 [hep-ex/0405071].

[28] **BaBar** Collaboration, J. Lees *et. al.*, *Improved Limits on B^0 Decays to Invisible Final States and to $\nu\bar{\nu}\gamma$*, *Phys.Rev.* **D86** (2012) 051105 [1206.2543].

[29] **Belle** Collaboration, C. Hsu *et. al.*, *Search for B^0 decays to invisible final states*, *Phys.Rev.* **D86** (2012) 032002 [1206.5948].

[30] L. Borissov, J. M. Conrad and M. Shaevitz, *Searching for the lightest neutralino at fixed target experiments*, hep-ph/0007195.

[31] **NuTeV Collaboration** Collaboration, T. Adams *et. al.*, *Observation of an anomalous number of dimuon events in a high-energy neutrino beam*, *Phys.Rev.Lett.* **87** (2001) 041801 [hep-ex/0104037].

[32] **D0** Collaboration, V. Abazov *et. al.*, *Search for neutral, long-lived particles decaying into two muons in $p\bar{p}$ collisions at $\sqrt{s}$ = 1.96-TeV*, *Phys.Rev.Lett.* **97** (2006) 161802 [hep-ex/0607028].

[33] L. Okun, *Mirror particles and mirror matter: 50 years of speculations and search*, *Phys.Usp.* **50** (2007) 380–389 [hep-ph/0606202].

[34] M. Baumgart, C. Cheung, J. T. Ruderman, L.-T. Wang and I. Yavin, *Non-Abelian Dark Sectors and Their Collider Signatures*, *JHEP* **0904** (2009) 014 [0901.0283].

[35] T. Beranek and M. Vanderhaeghen, *Study of the discovery potential for hidden photon emission at future electron scattering fixed target experiments*, 1311.5104.

[36] J. Bluemlein and J. Brunner, *New Exclusion Limits on Dark Gauge Forces from Proton Bremsstrahlung in Beam-Dump Data*, 1311.3870.

[37] S. Gninenko, *Constraints on sub-GeV hidden sector gauge bosons from a search for heavy neutrino decays*, *Phys.Lett.* **B713** (2012) 244–248 [1204.3583].

[38] S. Andreas, S. Donskov, P. Crivelli, A. Gardikiotis, S. Gninenko *et. al.*, *Proposal for an Experiment to Search for Light Dark Matter at the SPS*, 1312.3309.

[39] T. Appelquist and R. Shrock, *Neutrino masses in theories with dynamical electroweak symmetry breaking*, *Phys.Lett.* **B548** (2002) 204–214 [hep-ph/0204141].

[40] T. Appelquist, M. Piai and R. Shrock, *Fermion masses and mixing in extended technicolor models*, *Phys.Rev.* **D69** (2004) 015002 [hep-ph/0308061].

[41] T. Appelquist and R. Shrock, *Dynamical symmetry breaking of extended gauge symmetries*, *Phys.Rev.Lett.* **90** (2003) 201801 [hep-ph/0301108].

[42] S. Khalil and O. Seto, *Sterile neutrino dark matter in B - L extension of the standard model and galactic 511-keV line*, *JCAP* **0810** (2008) 024 [0804.0336].

[43] S. K. Kang and C. Kim, *Extended double seesaw model for neutrino mass spectrum and low scale leptogenesis*, *Phys.Lett.* **B646** (2007) 248–252 [hep-ph/0607072].

[44] K. L. McDonald, *Light Neutrinos from a Mini-Seesaw Mechanism in Warped Space*, *Phys.Lett.* **B696** (2011) 266–272 [1010.2659].

[45] M. Duerr, D. P. George and K. L. McDonald, *Neutrino Mass and $\mu \to e + \gamma$ from a Mini-Seesaw*, *JHEP* **1107** (2011) 103 [1105.0593].

[46] V. V. Khoze and G. Ro, *Leptogenesis and Neutrino Oscillations in the Classically Conformal Standard Model with the Higgs Portal*, *JHEP* **1310** (2013) 075 [1307.3764].

[47] T. Araki and Y. Li, *Q_6 flavor symmetry model for the extension of the minimal standard model by three right-handed sterile neutrinos*, *Phys.Rev.* **D85** (2012) 065016 [1112.5819].

[48] A. Merle and V. Niro, *Deriving Models for keV sterile Neutrino Dark Matter with the Froggatt-Nielsen mechanism*, *JCAP* **1107** (2011) 023 [1105.5136].

[49] K. Allison, *Dark matter, singlet extensions of the nuMSM, and symmetries*, *JHEP* **1305** (2013) 009 [1210.6852].

[50] L. Canetti, M. Drewes and M. Shaposhnikov, *Sterile Neutrinos as the Origin of Dark and Baryonic Matter*, *Phys.Rev.Lett.* **110** (2013), no. 6 061801 [1204.3902].

[51] M. Drewes and B. Garbrecht, *Leptogenesis from a GeV Seesaw without Mass Degeneracy*, *JHEP* **1303** (2013) 096 [1206.5537].

[52] M. Shaposhnikov, *Baryogenesis*, *J.Phys.Conf.Ser.* **171** (2009) 012005.

[53] D. Gorbunov and A. Panin, *On the minimal active-sterile neutrino mixing in seesaw type I mechanism with sterile neutrinos at GeV scale*, 1312.2887.

[54] S. Dodelson and L. M. Widrow, *Sterile-neutrinos as dark matter*, *Phys. Rev. Lett.* **72** (1994) 17–20 [hep-ph/9303287].

[55] X.-D. Shi and G. M. Fuller, *A new dark matter candidate: Non-thermal sterile neutrinos*, *Phys. Rev. Lett.* **82** (1999) 2832–2835 [astro-ph/9810076].

[56] K. Abazajian, G. M. Fuller and M. Patel, *Sterile neutrino hot, warm, and cold dark matter*, *Phys. Rev.* **D64** (2001) 023501 [astro-ph/0101524].

[57] K. Abazajian, G. M. Fuller and W. H. Tucker, *Direct detection of warm dark matter in the X-ray*, *Astrophys.J.* **562** (2001) 593–604 [astro-ph/0106002].

[58] J. den Herder, A. Boyarsky, O. Ruchayskiy, K. Abazajian, C. Frenk *et. al.*, *The Search for decaying Dark Matter*, 0906.1788.

[59] A. Boyarsky, D. Iakubovskyi and O. Ruchayskiy, *Next decade of sterile neutrino studies*, *Phys.Dark Univ.* **1** (2012) 136–154 [1306.4954].

[60] N. Terasawa, M. Kawasaki and K. Sato, *Radiative Decay of Neutrino and Primordial Nucleosynthesis*, *Nucl.Phys.* **B302** (1988) 697–738.

[61] A. Dolgov, S. Hansen, G. Raffelt and D. Semikoz, *Heavy sterile neutrinos: Bounds from big bang nucleosynthesis and SN1987A*, *Nucl.Phys.* **B590** (2000) 562–574 [hep-ph/0008138].

[62] A. D. Dolgov, S. H. Hansen, G. Raffelt and D. V. Semikoz, *Cosmological and astrophysical bounds on a heavy sterile neutrino and the KARMEN anomaly*, *Nucl. Phys.* **B580** (2000) 331–351 [hep-ph/0002223].

[63] A. Dolgov and F. Villante, *BBN bounds on active sterile neutrino mixing*, *Nucl.Phys.* **B679** (2004) 261–298 [hep-ph/0308083].

[64] G. M. Fuller, C. T. Kishimoto and A. Kusenko, *Heavy sterile neutrinos, entropy and relativistic energy production, and the relic neutrino background*, 1110.6479.

[65] O. Ruchayskiy and A. Ivashko, *Restrictions on the lifetime of sterile neutrinos from primordial nucleosynthesis*, *JCAP* **1210** (2012) 014 [1202.2841].

[66] P. Hernandez, M. Kekic and J. Lopez-Pavon, *Low-scale seesaw models versus $N_{\rm eff}$*, 1311.2614.

[67] G. Gelmini, E. Osoba, S. Palomares-Ruiz and S. Pascoli, *MeV sterile neutrinos in low reheating temperature cosmological scenarios*, *JCAP* **0810** (2008) 029 [0803.2735].

[68] F. Bezrukov, H. Hettmansperger and M. Lindner, *keV sterile neutrino Dark Matter in gauge extensions of the Standard Model*, *Phys.Rev.* **D81** (2010) 085032 [0912.4415].

[69] G. M. Fuller, A. Kusenko and K. Petraki, *Heavy sterile neutrinos and supernova explosions*, *Phys.Lett.* **B670** (2009) 281–284 [0806.4273].

[70] R. Alonso, M. Dhen, M. Gavela and T. Hambye, *Muon conversion to electron in nuclei in type-I seesaw models*, *JHEP* **1301** (2013) 118 [1209.2679].

[71] F. Bezrukov, *nu MSM-predictions for neutrinoless double beta decay*, *Phys.Rev.* **D72** (2005) 071303 [hep-ph/0505247].

[72] M. Blennow, E. Fernandez-Martinez, J. Lopez-Pavon and J. Menendez, *Neutrinoless double beta decay in seesaw models*, *JHEP* **1007** (2010) 096 [1005.3240].

[73] M. Mitra, G. Senjanovic and F. Vissani, *Heavy Sterile Neutrinos and Neutrinoless Double Beta Decay*, 1205.3867.

[74] S. Pascoli, M. Mitra and S. Wong, *The Effect of Cancellation in Neutrinoless Double Beta Decay*, 1310.6218.

[75] **LBNE** Collaboration, T. Akiri *et. al.*, *The 2010 Interim Report of the Long-Baseline Neutrino Experiment Collaboration Physics Working Groups*, 1110.6249.

[76] J. C. Helo, S. Kovalenko and I. Schmidt, *On sterile neutrino mixing with ν_τ*, *Phys.Rev.* **D84** (2011) 053008 [1105.3019].

[77] L. Lello and D. Boyanovsky, *Searching for sterile neutrinos from π and K decays*, *Phys.Rev.* **D87** (2013) 073017 [1208.5559].

[78] L. Lello and D. Boyanovsky, *Charged lepton mixing via heavy sterile neutrinos*, 1212.4167.

[79] I. M. Shoemaker, K. Petraki and A. Kusenko, *Collider signatures of sterile neutrinos in models with a gauge-singlet Higgs*, *JHEP* **1009** (2010) 060 [1006.5458].

[80] J. C. Helo, S. Kovalenko and I. Schmidt, *Sterile neutrinos in lepton number and lepton flavor violating decays*, *Nucl.Phys.* **B853** (2011) 80–104 [1005.1607].

[81] A. Shaykhiev, Y. Kudenko and A. Khotyantsev, *Searches for heavy neutrinos in the decays of positively charged kaons*, *Phys.Atom.Nucl.* **74** (2011) 788–793.

[82] C. Wendt, G. Abrams, D. Amidei, A. Baden, T. Barklow *et. al.*, *Search for Heavy Neutrino Production at PEP*, *Phys.Rev.Lett.* **58** (1987) 1810.

[83] D. Gorbunov and M. Shaposhnikov, *How to find neutral leptons of the nuMSM?*, *JHEP* **0710** (2007) 015 [0705.1729].

[84] S. Ramazanov, *Semileptonic decays of charmed and beauty baryons with sterile neutrinos in the final state*, *Phys.Rev.* **D79** (2009) 077701 [0810.0660].

[85] G. Cvetic, C. Dib and C. Kim, *Probing Majorana neutrinos in rare $\pi^+ \to e^+e^+\mu^-\nu$ decays*, *JHEP* **1206** (2012) 149 [1203.0573].

[86] G. Cvetic, C. Dib, S. K. Kang and C. Kim, *Probing Majorana neutrinos in rare K and D, D_s, B, B_c meson decays*, *Phys.Rev.* **D82** (2010) 053010 [1005.4282].

[87] A. Kusenko, S. Pascoli and D. Semikoz, *New bounds on MeV sterile neutrinos based on the accelerator and Super-Kamiokande results*, *JHEP* **0511** (2005) 028 [hep-ph/0405198].

[88] D. Britton, S. Ahmad, D. Bryman, R. Burnham, E. Clifford *et. al.*, *Improved search for massive neutrinos in pi+ → e+ neutrino decay*, *Phys.Rev.* **D46** (1992) 885–887.

[89] **PIENU** Collaboration, M. Aoki *et. al.*, *Search for Massive Neutrinos in the Decay $\pi \to e\nu$*, *Phys.Rev.* **D84** (2011) 052002 [1106.4055].

[90] R. Hayano, T. Taniguchi, T. Yamanaka, T. Tanimori, R. Enomoto *et. al.*, *HEAVY NEUTRINO SEARCH USING K(mu2) DECAY*, *Phys.Rev.Lett.* **49** (1982) 1305.

[91] G. Bernardi, G. Carugno, J. Chauveau, F. Dicarlo, M. Dris *et. al.*, *Search for Neutrino Decay*, *Phys.Lett.* **B166** (1986) 479.

[92] G. Bernardi, G. Carugno, J. Chauveau, F. Dicarlo, M. Dris *et. al.*, *FURTHER LIMITS ON HEAVY NEUTRINO COUPLINGS*, *Phys.Lett.* **B203** (1988) 332.

[93] **NuTeV, E815** Collaboration, A. Vaitaitis *et. al.*, *Search for neutral heavy leptons in a high-energy neutrino beam*, *Phys.Rev.Lett.* **83** (1999) 4943–4946 [hep-ex/9908011].

[94] **CHARM** Collaboration, F. Bergsma *et. al.*, *A Search for Decays of Heavy Neutrinos in the Mass Range 0.5-GeV to 2.8-GeV*, *Phys.Lett.* **B166** (1986) 473.

[95] **NOMAD** Collaboration, P. Astier *et. al.*, *Search for heavy neutrinos mixing with tau neutrinos*, *Phys.Lett.* **B506** (2001) 27–38 [hep-ex/0101041].

[96] R. Shrock, *New Tests For, and Bounds On, Neutrino Masses and Lepton Mixing*, *Phys.Lett.* **B96** (1980) 159.

[97] R. E. Shrock, *General Theory of Weak Leptonic and Semileptonic Decays. 1. Leptonic Pseudoscalar Meson Decays, with Associated Tests For, and Bounds on, Neutrino Masses and Lepton Mixing*, *Phys.Rev.* **D24** (1981) 1232.

[98] R. E. Shrock, *General Theory of Weak Processes Involving Neutrinos. 2. Pure Leptonic Decays*, *Phys.Rev.* **D24** (1981) 1275.

[99] R. E. Shrock, *Pure Leptonic Decays With Massive Neutrinos and Arbitrary Lorentz Structure*, *Phys.Lett.* **B112** (1982) 382.

[100] A. Atre, T. Han, S. Pascoli and B. Zhang, *The Search for Heavy Majorana Neutrinos*, *JHEP* **0905** (2009) 030 [0901.3589].

[101] **NA3** Collaboration, J. Badier *et. al.*, *Mass and Lifetime Limits on New Longlived Particles in 300-GeV/cπ^- Interactions*, *Z.Phys.* **C31** (1986) 21.

[102] **WA66** Collaboration, A. M. Cooper-Sarkar *et. al.*, *Search for Heavy Neutrino Decays in the BEBC Beam Dump Experiment*, *Phys.Lett.* **B160** (1985) 207.

[103] **FMMF** Collaboration, E. Gallas *et. al.*, *Search for neutral weakly interacting massive particles in the Fermilab Tevatron wide band neutrino beam*, *Phys.Rev.* **D52** (1995) 6–14.

[104] **CHARM II** Collaboration, P. Vilain *et. al.*, *Search for heavy isosinglet neutrinos*, *Phys.Lett.* **B343** (1995) 453–458.

[105] **DELPHI** Collaboration, P. Abreu *et. al.*, *Search for neutral heavy leptons produced in Z decays*, *Z.Phys.* **C74** (1997) 57–71.

[106] **L3** Collaboration, O. Adriani *et. al.*, *Search for isosinglet neutral heavy leptons in Z0 decays*, *Phys.Lett.* **B295** (1992) 371–382.

[107] **Belle** Collaboration, D. Liventsev *et. al.*, *Search for heavy neutrinos at Belle*, *Phys.Rev.* **D87** (2013) 071102 [1301.1105].